ADVANCED ENERGY MATERIALS

Supporting Information

for *Adv. Energy Mater.,* DOI: 10.1002/aenm.201902819

Stable Li Metal Anode Enabled by Space Confinement and Uniform Curvature through Lithiophilic Nanotube Arrays

Karnpiwat Tantratian, Daxian Cao, Ahmed Abdelaziz, Xiao Sun, Jinzhi Sheng, Avi Natan, Lei Chen, and Hongli Zhu**

Supporting Information

Stable Li Metal Anode Enabled by Space Confinement and Uniform Curvature through Lithiophilic Nanotube Arrays

Karnpiwat Tantratian[2,†], Daxian Cao[1,†], Ahmed Abdelaziz[1], Xiao Sun[1], Jinzhi Sheng[1], Avi Natan[1], Lei Chen[2,], Hongli Zhu[1,*]*

[1]Department of Mechanical and Industrial Engineering, Northeastern University, Boston, Massachusetts 02115, United States.

[2]Department of Mechanical Engineering, University of Michigan-Dearborn, Dearborn, Michigan 48128-1491, United States.

* Corresponding author: Hongli Zhu E-mail: h.zhu@neu.edu

Lei Chen E-mail: leichn@umich.edu

† These authors contributed equally to this work.

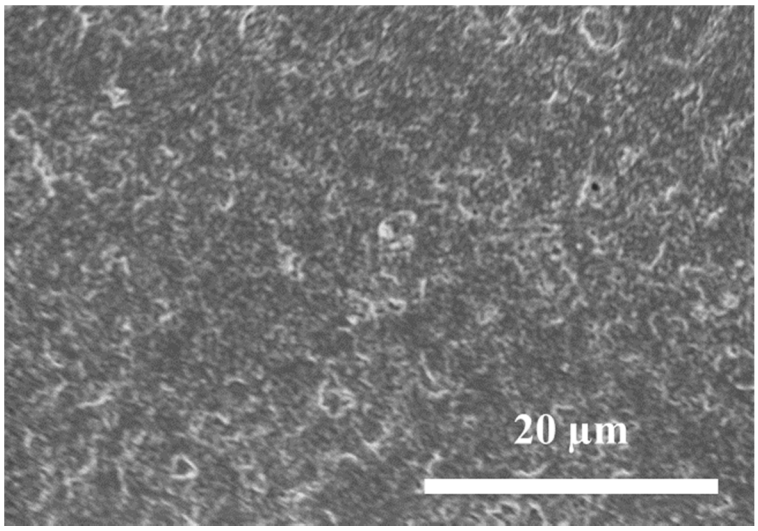

Figure S1. The surface morphology of the pristine Li foil before cycling.

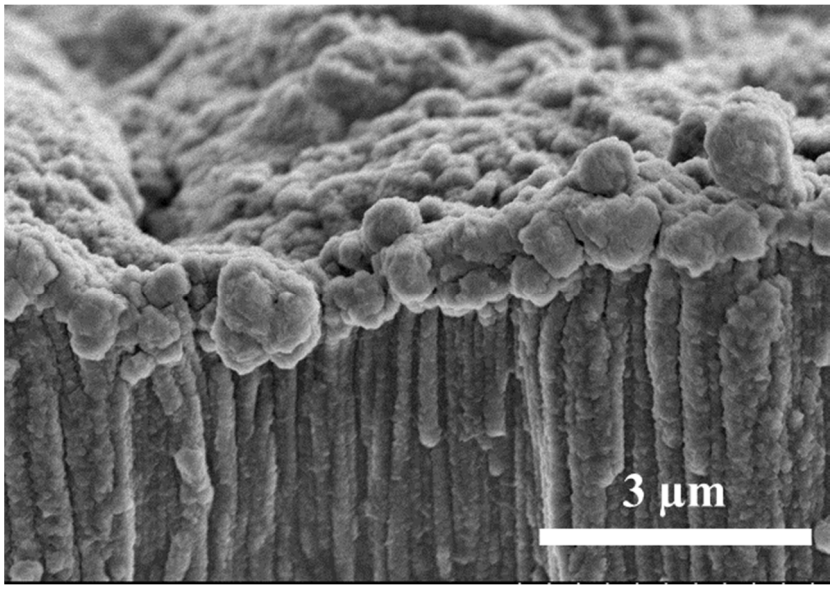

Figure S2. The morphology of Li deposition on the closed Li nanotube after cycling.

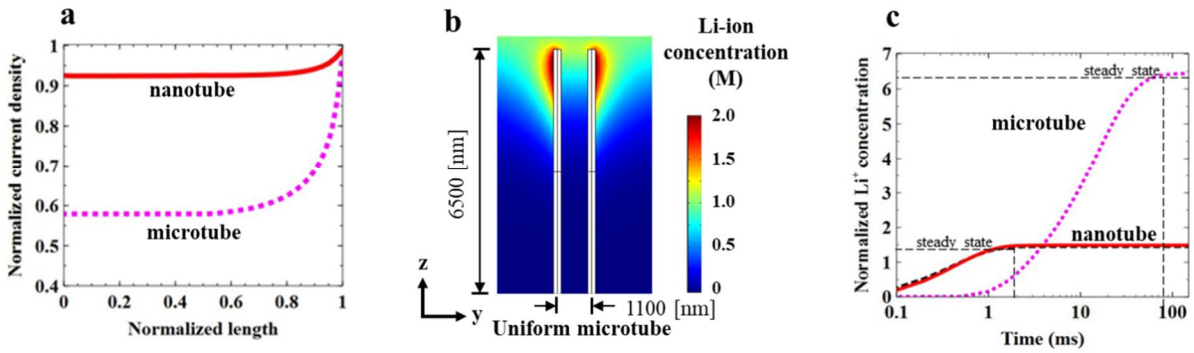

Figure S3. The current density simulation results of uniform microtubes sample. a) Plot of normalized current density along the tube length for uniform nanotube and microtube. b) The Li-ion concentration distribution on a 2D cut-plane along the uniform microtube wall at t_0 = 5 ms. c) Plot of time against Li-ion concentration at the middle of the tubes for 2 different cases.

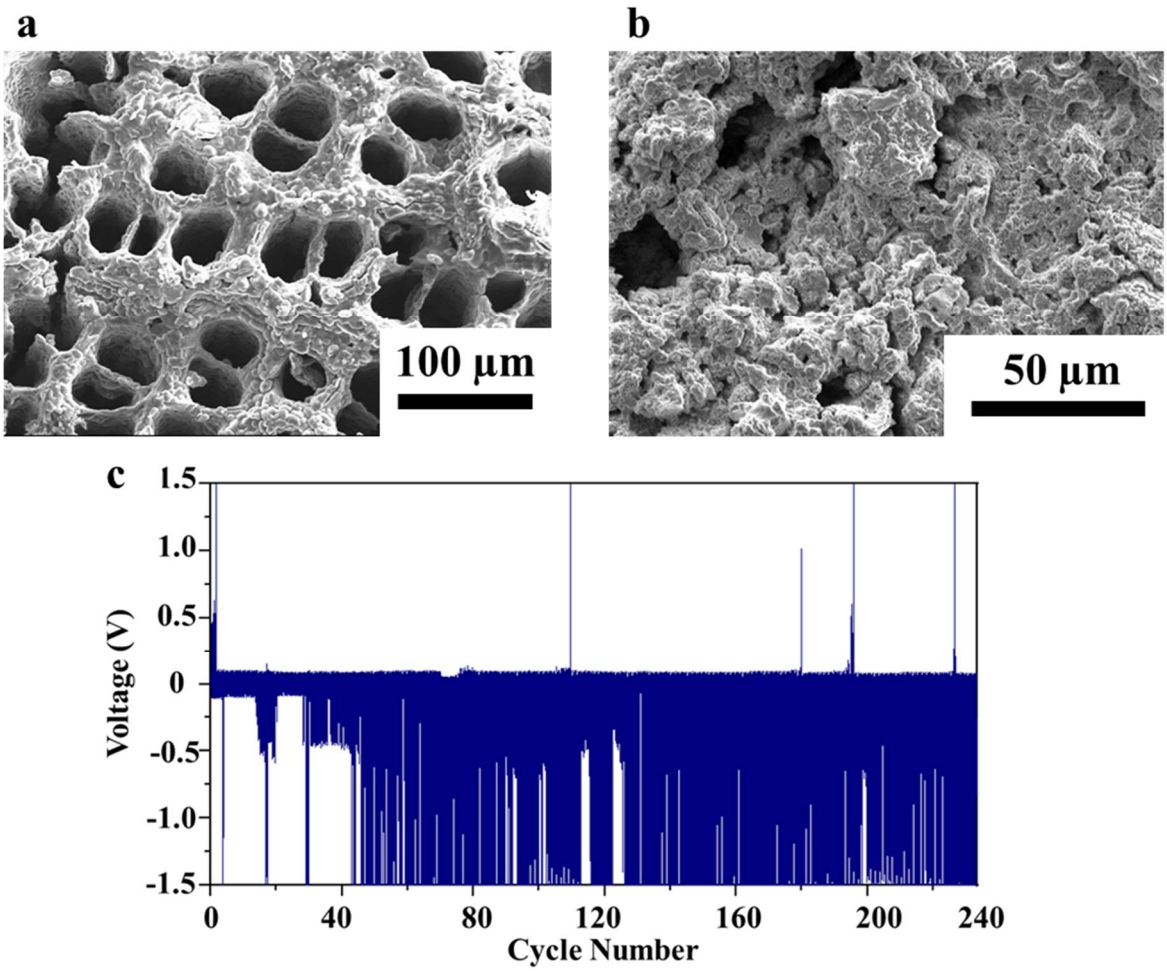

Figure S4. Characterization and electrochemical performance of hollow C-wood as a host structure for Li metal anode. SEM images of the Li metal anode based on a wood scaffold a) before and b) after 100 cycles. c) Symmetric cells electrochemical measurement cycling at a current density of 4 mA cm^{-2} and cycling capacity 4 mA h cm^{-2}.

Phase-field Modeling for Electrodeposition

In this work, the non-linear phase-field model, developed by L. Chen,[12] is used to simulate the evolution of Li plating on the electrode surface. The model accounts for the electrochemical reaction kinetics at the surface of the electrode ($Li^+ + e \rightarrow Li$). The phase-field parameter (ξ), which continuously varies from 0 to 1, is used to differentiate between the Li metal electrode ($\xi = 1$) and the electrolyte ($\xi = 0$). The morphological evolution of Li plating is governed by Allen-Cahn equation integrating Butler-Vomer kineties, expressed as

$$\frac{\partial \xi}{\partial t} = -L_\sigma(g'(\xi) - \kappa\nabla^2\xi) - L_\eta g'(\xi)\left\{\exp\left[\frac{(1-\alpha)nF\eta_a}{RT}\right] - c_+\exp\left[\frac{-\alpha nF\eta_a}{RT}\right]\right\}, \quad (1)$$

where $h(\xi) = \xi^3(6\xi^2 - 15\xi^3 + 10)$ is an interpolating function, L_σ and L_η are the interface mobility and the reaction-related constant, respectively, η_a is the activation overpotential. The first and second term on the right-hand side (RHS) of Equation 1 are related to the driving force due to the interfacial energy and electrochemical reactions, respectively. Equation 1 is solved simultaneously with mass and charge conservation equations, which can be written as

$$\frac{\partial c_+}{\partial t} = \nabla \cdot \left[D^{eff}\nabla c_+ + \frac{D^{eff}\nabla c_+}{RT} nF\nabla\phi\right] - \frac{c_s}{c_0}\frac{\partial \xi}{\partial t}, \quad (2)$$

$$\nabla \cdot [\sigma^{eff}\nabla\phi] = I_R, \quad (3)$$

where $D^{eff} = D^e h(\xi) + D^s(1 - h(\xi))$ is the effective diffusion coefficient, D^e and D^s are the Li-ion diffusion coefficients in the electrode, and in the electrolyte, respectively, $\sigma^{eff} = \sigma^e h(\xi) + \sigma^s(1 - h(\xi))$ is the effective conductivity, and σ^e and σ^s are the conductivities of electrode and the electrolyte solutions, respectively. In Equation 3, the source term $I_R = nFc_s\partial\xi/\partial t$ is associated with charges leaving/entering due to the reaction rate. The Li plating was simulated on COMSOL Multiphysics 5.3, employing the finite element method. We chose the adaptive mesh with small enough minimum grid spacing to effectively capture the moving

interface. For the spaced Li nanotubes, the tube diameter, the tube length and the inter-nanotube space were 90 nm, 650 nm, and 150 nm, respectively (**Figure S5**). For the closed Li nanotubes, the tube spacing was reduced to 50 nm. However, for Li foil, the domain size was 4.0 x 4.0 μm. Simulation parameters are listed in **Table S1**. For initial conditions, the uniform Li nucleation sites were applied over the nanotube surfaces due to the uniform current density distribution near the nanotube walls. However, a few Li metal perturbations, resulting from the large volume change during cycling, were designed on the Li foil surface. The initial Li-ion concentration in the electrolyte domain is 1.0 M, while the initial Li-ion in the electrode was absent, 0.0 M. The initial electric potential in the electrolyte domain and Li metal were 0.1 V, and 0.0 V, respectively. The Dirichlet boundary conditions for Equation 2 and Equation 3 were only employed at the opposite side of the electrode with the Li-ion concentration of 1.0 M and the electric potential of 0.1 V, respectively, to represent the bulk electrolytes. The electric potential of 0.1 V is chosen based on the magnitude of measured overpotential in electrochemical measurements at the first few cycles. The plots in Figure 4 are captured at the simulation time of 800 s.

Current Density Distribution Modeling

The secondary current distribution, which is a built-in model in COMSOL Multiphysics 5.3, is used to predict the current density and electric potential distributions in the electrolyte. The model assumes that in the electrolyte the charge transfer obeys Ohm's law, that is

$$i = -\sigma \nabla \phi, \tag{4}$$

where i is the current density, σ is the conductivity, and ϕ is the electric potential. The model considers the activation overpotential, $\eta_a = \Delta\phi - E^{\Theta}$, where $\Delta\phi$, and E^{Θ} are the potential difference at the interface and the standard half-cell potential, respectively. The Butler-Volmer equation was chosen to describe the relationship between the overpotential and current density at the electrode interface, expressed as

$$j = j_0 \left(\exp\left[\frac{(1-\alpha) z F \eta_a}{RT}\right] - \exp\left[\frac{-\alpha z F \eta_a}{RT}\right] \right), \tag{5}$$

where j is the charge transfer current density, j_0 is the exchange current density, α is the cathodic charge transfer coefficient. The current density (j) was simply used to describe the boundary condition related to electrochemical reaction at the electrode surface, $n \cdot i = j$. Lastly, Equation 4 was solved together with Nernst-Planck equation to predict ions movement under migration and diffusion in the dilute electrolyte, which can be written as

$$\frac{\partial c_+}{\partial t} = \nabla \cdot \left[D \nabla c_+ + z \frac{D c_+}{RT} F \nabla \phi \right], \tag{6}$$

where c_+, z, and D denote the Li-ion concentration, charge number and diffusion coefficient, respectively. For meshing, the very fine mesh size was applied on the electrode surface where the gradient of current density likely occurred. A uniform nanotube had the inner and outer radius of 35 and 45 nm (for skeleton), respectively, with the Li metal layer of 10 nm covering the outer surface. A non-uniform nanotube was randomly designed with extremely

non-uniform curvatures. For both cases, the length of the tubes was 650 nm. For simplicity, only movement of Li-ions was considered. The Li-ion diffusion coefficient was 0.9×10^{-9} m^2 s^{-1}. The exchange current density (j_0), and cathodic charge transfer coefficient were assumed to be 500 A/m^2, and 0.5, respectively. The electrode surface areas were selected as shown in **Figure S6**, with the designed electric potential of -1.25 V, while the rest of the surfaces were insulated. We considered no ion flux moving in/out the electrolyte boundary, except at the top boundary where a constant Li-ion concentration of 1 M is set. Lastly, for the initial condition, the electrolyte potential, and Li-ion concentration are assumed to 0 V, and 0 M, respectively.

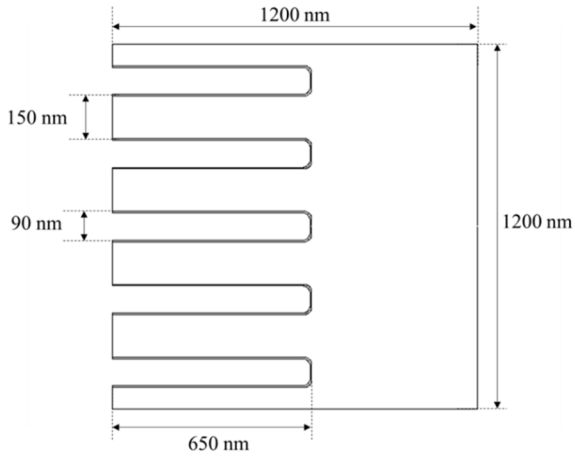

Figure S5 2D nanotube geometry used in phase-field electrodeposition modeling.

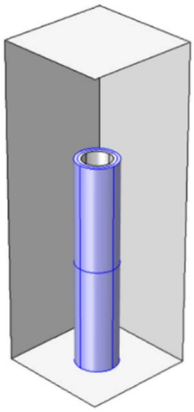

Figure S6 3D geometry of the uniform nanotube used in current density distribution modeling.

Table S1. Simulation parameters used in phase-field electrodeposition modeling.

Parameters	Value	Normalized value
Gradient energy coefficient, κ	1.5 x 10^{-5} (J m^{-1})	0.01
Li^+ diffusivity in liquid, D^s_{Li+}	9.0 x 10^{-10} (m^2 s^{-1})	180
Li^+ diffusivity in electrode, D^e_{Li+}	9.0 x 10^{-13} (m^2 s^{-1})	0.18
Electrolyte conductivity, σ^s	1 (S m^{-1})	100
Electrode conductivity, σ^e	1 x 10^7 (S m^{-1})	10^9
Interfacial mobility, L_σ	1.33 x 10^{-5} (m^3 J^{-1} s^{-1})	200
Reaction-related constant, L_η	0.02 (s^{-1})	400